FINAL PUBLISHABLE REPORT

Grant Agreement number	15SIB03
Project short name	OC18
Project full title	Optical clocks with 1E-18 uncertainty

Project start date and duration:	01 May 2016, 36 months	
Coordinator: Rachel Godun, Dr., NPL	Tel:+44 20 8943 6072	E-mail: rachel.godun@npl.co.uk
Project website address: www.OC18.eu		
Internal Funded Partners: 1. NPL, United Kingdom 2. CMI, Czech Republic 3. INRIM, Italy 4. LNE, France 5. OBSPARIS, France 6. PTB, Germany 7. TUBITAK, Turkey 8. VTT, Finland	External Funded Partners: 9. KU, Denmark 10. LUH, Germany 11. UMK, Poland	Unfunded Partners: 12.

TABLE OF CONTENTS

1 Overview

This project has made significant advances in the performance of optical atomic clocks across Europe, to support the ongoing work towards a redefinition of the SI second. World-leading developments from this project in laser frequency stabilisation and atom trapping have brought about improvements in both the accuracy and stability of the clocks. This measurement capability enables the clocks to generate optical frequencies with reduced uncertainty for end users in metrology and industry. The clocks have also been used for scientific measurements that test the laws of fundamental physics at unprecedented levels.

2 Need

There has been a need for optical clocks with fractional frequency uncertainty at the 10^{-18} level from a wide range of sectors including basic science and metrology to applications in geodesy, satellite navigation and environmental monitoring.

It has been anticipated in the metrology community that there will be an international decision to redefine the SI second in terms of an optical standard, since optical clocks have already been shown to outperform the caesium primary standards by more than an order of magnitude. Before a redefinition can be made, however, there must be confidence that the optical clocks actually perform at the level they are estimated to achieve. Measurements must therefore be carried out to validate the performance, using the highest accuracy clocks available. Tests of fundamental science, such as looking for violations of Einstein's Equivalence Principle, also require high-accuracy clocks to set tighter constraints on physical theories. There is therefore a need for fractional frequency uncertainties arising from systematic shifts to reach down to the 10^{-18} level.

For statistical uncertainties to reach the same level, the frequency output from optical clocks must be averaged over a period of time. A barrier to industry using optical clocks 'in the field' has been that the necessary averaging time was of the order of days or weeks. For geodesy applications such as monitoring changes in ocean currents or surveying for gas and oil, much shorter averaging times are required. To reach statistical uncertainties of 10^{-18} after just a few hours, laser frequency instabilities need to be at or below 10^{-16} at 1 s. New atom traps that can support long coherent probe times (> 1 s) are also needed so that frequency instability is not degraded when probing the atoms.

3 Objectives

The main aim of this project is to develop world-leading optical atomic clocks across Europe, which will support a future redefinition of the SI second and underpin international time scales.

1. To achieve instabilities in laser frequencies of 1×10^{-16} or below after 1 s, by investigating: (a) room temperature glass cavities, (b) cryogenic silicon cavities (c) spectral hole burning and (d) active resonators. Guidelines will be written to show how this stability can be transferred from the laser source to the atoms in optical clocks whilst adding no more than 1×10^{-17} to the laser noise after 1 s.
2. To develop traps for single ions and neutral atoms that support > 1 s probe times. Guidelines will be written for an optimised design of ion trap; for neutral atoms a report will be written summarising the effects of collisions, photon scattering and parametric heating on coherence times.
3. To evaluate and reduce systematic uncertainties in optical clocks to the level of 10^{-18}. A report will be written summarising improved control and measurement of the thermal environment in single ion and neutral atom optical clocks, leading to 10^{-18} uncertainties in blackbody radiation shifts for clocks operating at both cryogenic and room temperatures. An uncertainty report for controlling and evaluating lattice light shifts and collisional shifts at the 10^{-18} level in neutral atom optical lattice clocks will also be written.
4. To implement novel interrogation methods in optical clocks that use an optimised sequence of probe pulses to reduce even further the instability and inaccuracy of the clocks. To validate performance with target uncertainty 1×10^{-18}, through direct measurement of the frequency difference between two independent clocks.

4 Results

4.1 Objective 1 - Laser frequency instabilities and frequency transfer to atoms

4.1.1 Laser frequency instabilities (Objective 1)

Ultrastable lasers are a key component in optical atomic clocks. They serve as the interrogation laser for atomic clock transitions and largely determine the stability of the clocks. Given the narrow natural linewidth of optical clock transitions, it is the frequency fluctuations and coherence time of the lasers that tend to limit the resolvable linewidth. Due to the discontinuous interrogation, the laser's frequency fluctuations also affect the clock stability via the Dick effect. Therefore great effort has been put into the realisation of laser sources with low frequency noise.

The most common method to stabilise laser frequencies has been with the use of passive, high-finesse Fabry-Perot cavities. With well-designed servo electronics, the fractional frequency instability of the laser is then identical to the fractional optical-path-length instability of the cavity. Accordingly, any environmental perturbation such as temperature fluctuations or vibrations which affect the optical path length must be suppressed to a level compatible with the target stability.

This project has investigated the performance that can be achieved with room-temperature glass cavities and demonstrated instabilities of 10^{-16} after 1 s [Didier2019]. Placing cavities in a cryogenic environment can further decrease the length fluctuations caused by Brownian thermal noise of the cavity components and so this project also investigated laser stabilisation to cavities made of single-crystal silicon at cryogenic temperatures. This approach reached laser instabilities of 4×10^{-17} [Matei2017] - a new state-of-the-art and a factor of two beyond the best previously reported results. Further investigations were also carried out at even colder temperatures of 4 K [Zhang2017].

In parallel, novel laser stabilisation techniques that do not require such extreme control of the length of a Fabry-Perot cavity were also explored: spectral hole burning [Gobron2017] and active resonators [Schäffer2017]. Both these frequency stabilisation methods rely on atomic transitions to set the frequency reference rather than cavity lengths. Results demonstrated laser frequency instabilities of ~ 1×10^{-15} at 1 s. Whilst these techniques are still in their infancy, it is foreseeable that these stabilisation techniques may surpass the results achieved with the best optical cavities.

Further details and results for each of these different approaches to laser stabilisation is given in the sections below:

Room-temperature glass cavities

A simple 30-cm long ultra-low-expansivity glass cavity with fused silica mirrors was developed for operation at 946 nm [Didier2019]. The cavity was rested on a simple vibration-insensitive support, such that fractional frequency changes due to accelerations were no more than a few 1×10^{-11} / ms^{-2} in all directions. An anti-vibration platform damped vibrations above 0.7 Hz, so that typical residual accelerations had an amplitude spectral density on the order of 1×10^{-5} / ms^{-2} /√Hz or below at all Fourier frequencies. The temperature control of the cavity was maintained by an inner gold-coated shield inside a vacuum chamber, which was itself surrounded by a temperature-controlled shield and a polystyrene enclosure. The time constant of this setup, in reaction to a 0.5°C temperature step, was 91 hours, which gave excellent damping of external perturbations. Finally, the electro-optic modulator producing the sidebands necessary for Pound-Drever-Hall locking was made from a Brewster-cut prism KTP crystal and the passive fractional residual amplitude modulation was below 2×10^{-6}. The resulting fractional frequency stability of the laser locked to this cavity was 1.1×10^{-16} at 1 s, corresponding to the limit imposed by the thermal noise.

Cryogenic silicon cavities

To tackle the limit imposed on the stability of cavity length by thermal noise, this project developed two 212-mm long cavities made from single-crystal silicon, operated at cryogenic temperatures, as shown in Figure 1, [Matei2017]. The choice of silicon was based on a very small mechanical loss factor (~10^{-8}) and a large Youngs Modulus (~200 GPa). Together, these result in very small atomic motion at a given energy. The cryogenic temperature then reduces the thermal energy in the system to restrict this motion even further. Both the cavity spacer and the mirror substrates were made from monolithic silicon crystals and the operating temperature was chosen to be 124 K, where the coefficient of thermal expansion exhibits a zero-crossing. The

experimental comparison of lasers locked to the two cavities revealed that each achieved a world-leading frequency stability floor of 4×10^{-17}, which is at the theoretical noise limit.

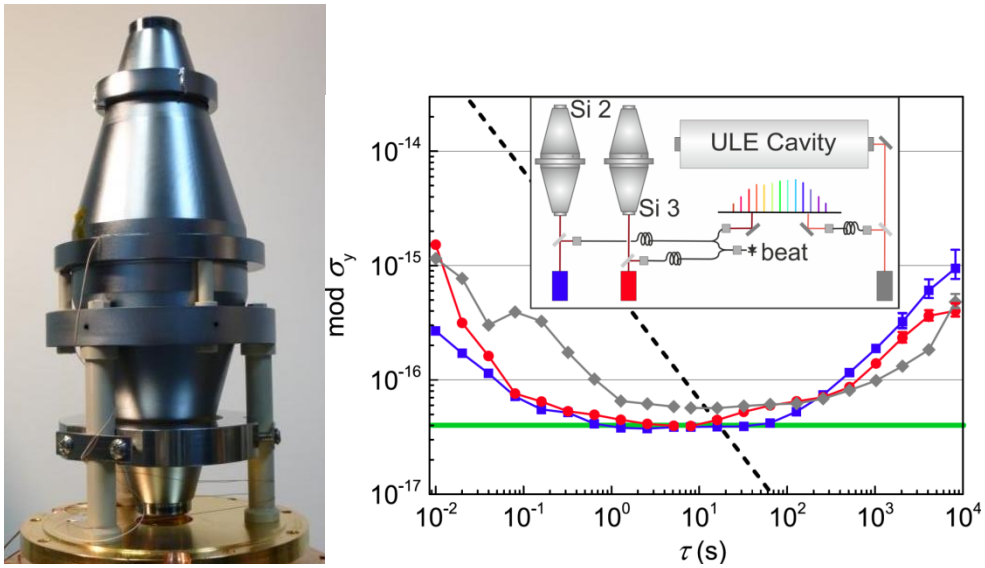

Figure 1: A vertically-mounted, 212-mm long silicon cavity is shown on the left and the corresponding fractional frequency instability achieved with this cavity is shown in the plot on the right. Graph reproduced from [Matei2017].

To push towards a cavity system with an even lower theoretical noise floor requires further reductions in temperature and/or materials that further restrict atomic motion. Work carried out in this project has made progress on both of these aspects. To demonstrate what can be achieved at even lower temperatures, a 60-mm long silicon cavity was operated at 4 K [Zhang2017] – another temperature where the coefficient of thermal expansion in silicon is zero. A major source of technical noise that had to be overcome was vibrations from the cyclic operation of the closed-cycle cryocooler that was needed to achieve the 4 K temperature. (The cryocooler had not been necessary for operation at 124 K because, in that case, cold nitrogen gas from a liquid nitrogen dewar was sufficient). The two-stage Gifford-McMahon cryocooler's vibrations were isolated as much as possible from the cavity by fixing the cryocooler to the concrete floor of the laboratory, separating the cold chamber from the main cryocooler by a vacuum bellows, and placing the cold chamber on an active vibration isolation table. A frequency instability floor of 1×10^{-16} was achieved, which was a ten-fold improvement in short-term instability over previous sub-10 K systems. To experiment with novel materials in the cavity design, the dielectric coatings that form the reflective surfaces on the silicon mirror substrates were replaced with crystalline mirror coatings. This new type of coating benefits from a loss angle that is 10 times lower than the one of dielectric coatings, and it is therefore a very promising technology to reduce the effects of thermal noise and reach even better stabilities. These coatings had previously been demonstrated to work at room-temperature, but it was unclear if cryogenic temperatures would damage them or would cause them to peel away from the mirror substrates. Tests proved, however, that the coatings could not only survive temperature cycling down to 100 K, but also that the finesse of the reflective coatings increased favourably from 300,000 at room temperature to 400,000 at the cryogenic temperature. These crystalline coatings will now be incorporated into the next generation of silicon cavities and thermal noise floors as low as 1×10^{-17} are anticipated.

Spectral hole burning

By stabilising a laser to an atomic reference instead of to a Fabry-Perot cavity, the fundamental limits imposed by thermal noise in the cavity length are no longer an issue. In spectral hole burning, the principle is to stabilise the laser to a narrow spectral feature in rare-earth doped crystals at cryogenic temperatures. Some rare-earth elements have metastable states with lifetimes of several days at temperatures of 4 K and below. Perturbations from the crystalline matrix in which these atoms are held lead to inhomogeneous broadening of the linewidth, up to a few GHz. By applying a narrow linewidth (< 100 Hz) laser in the inhomogeneously broadened absorption spectrum, resonant rare-earth atoms will be optically pumped into these metastable states. This generates a narrow spectral hole in the inhomogeneously broadened spectrum, which persists for several hours after extinction of the 'burning' laser. Subsequent laser probing of this narrow spectral feature

allows an error signal to be generated which can be used to frequency-lock the probing laser to the spectral hole frequency.

In this project, narrow spectral holes were burnt into the transmission spectrum of Eu^{3+} ions inserted in a crystalline matrix, operated at 4 K [Gobron2017]. The spectral features were as narrow as 4 kHz, so the system could be competitive with the best optical cavities. Frequency stabilities at the level of 1×10^{-15} at 1 s were achieved with an 1160-nm laser, frequency-doubled and locked to spectral holes. This is a first for Europe and within a factor of two of the world-leading results in this frequency stabilisation technique.

As with the cryogenic silicon cavity, vibrations from the pulsed-tube cryostat needed to be minimised. Copper-beryllium springs were added to improve the passive isolation of the rare-earth doped crystal from the main stage of the cryocooler, and an active servo stabilisation loop was also engaged to minimise the transmission of vibrations. The resulting frequency stability is no longer limited by vibrations, but by residual temperature fluctuations in the system.

Active resonators

Similarly to the spectral hole burning technique, the approach here was to make use of an atomic reference frequency to generate stable laser light. ^{88}Sr atoms were placed inside a low-finesse optical cavity and advantage was taken of atom-light coupling phenomena in cavities, with the narrow atomic transition dominating the frequency response of the system.

The work was carried out in two stages in this project. In the first stage, a laser was stabilised to the 7.6 kHz atomic feature in the ^{88}Sr $^1S_0$ – $^3P_1$ transition [Schäffer2017]. As shown in Figure 2, a cloud of atoms was prepared in a magneto-optical trap inside an optical cavity. Laser light at 689 nm was then sent into the cavity and acquired a frequency-dependent phase shift as it interacted with the atoms. The atom-light coupling, and hence the phase shift, was increased by a factor of the cavity finesse as the light was reflected back and forth in the cavity. Making use of the frequency dependence of this phase shift, an error signal was generated from the transmission signal through the cavity and used to lock the laser frequency to that of the atomic transition. The atoms were probed typically for 100 µs every 100 ms, limited by the time needed to reload the magneto-optical trap from one probe cycle to the next. Stabilities of 1×10^{-14} after 1000 s were observed, with the duty cycle currently limiting the feedback bandwidth. The cavity itself was shown to have only a small influence on the laser stabilisation, meaning that the system was robust towards cavity fluctuations, as intended.

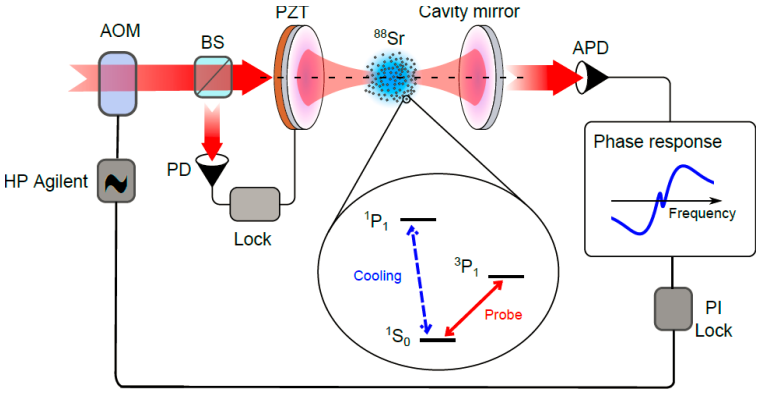

Figure 2: Cavity-based stabilisation to a narrow atomic feature. Demodulation of the light transmitted by the cavity leads to an error signal used to feedback to the frequency of the laser while the blue light necessary to form the magneto-optical trap is switched. Figure reproduced from [Schäffer2017].

In the second stage, the potential of atom-light coupling in a cavity to create a so-called 'active laser' was explored. The idea is to create the right conditions for the atoms to respond collectively such that when excited by a short pulse of radiation, they then emit a burst of light into the cavity mode. The linewidth of this superradiant light can be several orders of magnitude narrower than the atomic transition natural linewidth. This technique therefore has the potential to generate low frequency noise laser light, suitable for use in optical clocks. In this project, superradiant pulses of light were generated from about 10^7 atoms, cooled in a magneto-optical trap, and held within an optical cavity with finesse of 1200. The pulses lasted for 1.5 – 2 µs with several absorption and emission cycles taking place within the cavity. The details of the pulse duration, pulse power,

number of atoms etc. were all in excellent agreement with theoretical models that were developed. This work has therefore been a very promising step towards generating continuous superradiant light.

4.1.2 Transferring frequency stability from a laser source to the atoms (Objective 1)

Having produced laser sources with fractional frequency instabilities of 1 x 10^{-16} or below after 1 s, the next challenge is to be able to probe the reference atoms in the clock with laser light at the same frequency instability. This involves overcoming two problems:

The first problem is that ultrastable laser sources are often made in the infrared domain, due to the availability of narrow-linewidth lasers and the superior performance of Fabry-Perot cavities at these wavelengths. However, the atomic clock transition will generally be at an entirely different wavelength. The frequency stability must therefore be transferred from one laser wavelength to another. This is done using the so-called transfer oscillator method with optical frequency combs. Care must be taken that this process does not add more than 10^{-17} to the laser noise after 1 s otherwise the stability of the laser source will be degraded. More details about this are given below.

The second problem is that even if the frequency has been successfully transferred to the appropriate wavelength, the light must still propagate towards the atoms. The phase noise that is picked up along the entire optical path between the ultrastable laser and the atoms must therefore be compensated. This implies compensating the noise from propagation in optical fibres, in free space, in optical amplifiers, and in doubling crystals. Once again the target is not to add more than 10^{-17} to the laser noise after 1 s during the propagation to the atoms, and the results from this project are described in more detail below.

Transferring frequency stability from one laser wavelength to another

Optical frequency combs are commonly used in a transfer oscillator scheme to lock a slave laser at one wavelength to a master laser at a different wavelength. This can be accomplished with the frequency comb in either a single-branch setup, or a multi-branch setup. In the multi-branch approach, beat notes between the comb and the master laser on one hand, and between the comb and the slave laser on the other hand, are formed by independent optical amplifiers seeded by the light of the comb. This has the advantage that the beat notes can be optimised independently, but it comes at the expense of frequency noise: the differential noise between the optical amplifiers sets a limit to the stability of frequency transfer. In this project, a frequency comb based on an erbium-doped fibre laser was used in multi-branch mode to transfer frequency stability between lasers at 871 nm and 934 nm. The results are plotted in Figure 3(a), from which it can be seen that the fractional frequency instability measured between the beat notes at 871 nm and 934 nm achieved 1.5 x 10^{-17} at 1 s, an improvement of approximately one order of magnitude on the state-of-the-art at the start of the project. This success resulted from careful attention being paid to phase noise in the beat detection unit, and replacing fibre coupling into these units with free-space alignment.

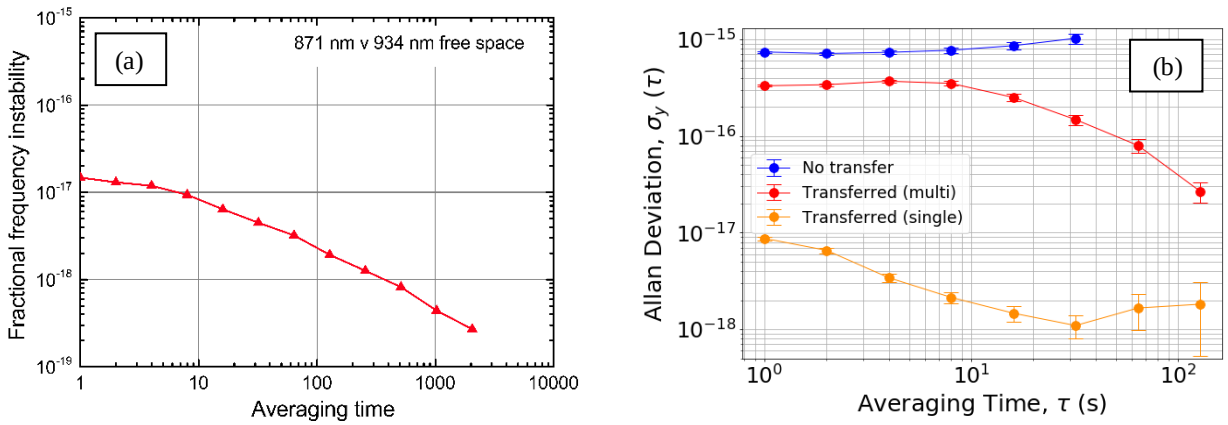

Figure 3: Fractional frequency instability after transfer across a frequency comb set up in (a) multi-branch mode between 871 nm and 934 nm and (b) single-branch mode between 1542 nm and 1062 nm shown in the orange plot.

Using the transfer oscillator scheme in the single-branch mode instead, all the beat notes are formed from the same optical output of the comb, allowing the comb parameters to be completely eliminated. This reduces the amount of noise added when frequencies are transferred from one wavelength to another. In this project, an

erbium-doped fiber-laser-based comb was used and transfer noise as low as 8 x 10^{-18} at 1 s was achieved between a 1542 nm laser and a 1062 nm laser, as shown in Figure 3(b). Similar results were also obtained for the stability transfer using the transfer oscillator method in single-branch mode between 1542 nm and 698 nm.

Transferring frequency stability along the propagation path to the atoms

Often, the atomic source in an optical clock is several metres of path length from the ultrastable laser source. The frequency stability must therefore be preserved as the light passes through elements such as optical fibres, amplifiers and doubling crystals [Rauf2018]. A typical frequency instability that might be picked up on short timescales (1 - 10 s) is 1 x 10^{-15} for a 10-metre long uncompensated fibre. In this project, strategies were developed that compensated noise in optical fibres down to 1 x 10^{-17} or below at 1 s using Michelson interferometers. Noise in optical amplifiers was compensated down to 4 x 10^{-17} at 1 s using Mach-Zehnder interferometers. It was also demonstrated with two independent systems that frequency doubling introduced a phase noise contributing no more than 1 x 10^{-17} at 1 s.

As the frequency stability of the laser source improves, longer probe times with less optical power are used to interrogate the atoms. With less optical power in the beam, it becomes increasingly difficult to set up an interferometric loop to stabilise the frequency. A theoretical study was therefore carried out for an alternative scheme to cancel the propagation noise. This alternative scheme relied on using a higher power beam at a frequency away from the atomic resonance to cancel the phase noise, but offset-locking the probe beam to the higher power beam so that its frequency noise properties would be the same. Calculations demonstrated that this technique should be successful and not hinder the accuracy budget beyond the target of 1 x 10^{-18}.

Conclusion for Objective 1

The key results for the first part of Objective 1 were demonstrations of laser frequency instabilities at the level of:

(a) 1 x 10^{-16} after 1 s for room-temperature glass cavities,
(b) 4 x 10^{-17} after 1 s for cryogenic silicon cavities,

making it clear that the target level of laser frequencies at 1 x 10^{-16} or below after 1 s has been met. New stabilisation techniques relying on spectral hole burning and active resonators were also explored, showing great promise for even lower frequency instabilities to be achieved in the future. A report was written, summarising all the laser instabilities achieved within this project.

The key results for the second part of Objective 1 were demonstrations of frequency transfer, increasing the frequency instability by no more than:

(a) 1.5 x 10^{-17} at 1 s using frequency combs in a multi-branch setup,
(b) 8 x 10^{-18} at 1 s using frequency combs in a single-branch setup.

It was also shown that the technical sources of noise that could affect the spatial transfer of light along the propagation path could be controlled at the 10^{-17} level or below at 1s, thus achieving the target set out in the objective. Guidelines were written, documenting in more detail the frequency transfer from the laser source to the atoms.

4.2 Objective 2 - Developing traps for single ions and neutral atoms that support > 1 s probe times

Long probe times are desirable in optical atomic clocks as this enables the best possible resolution of the atomic feature that is used to stabilise the optical frequency output of the clock. The maximum possible probe time is generally limited by either the loss of atoms from the trap, or else the loss of coherence in the atom-light coupling. The atom-light coherence can be affected by (i) laser frequency noise, (ii) atomic decoherence (e.g. through spontaneous decay after excitation by optical lattice photons), (iii) dephasing of the atomic interactions (e.g. from motional heating of trapped atoms leading to a spread of atom-light coupling strengths). Laser frequency noise was addressed by Objective 1, so Objective 2 therefore concentrated on atom loss, atomic decoherence, and dephasing of the atomic interactions.

The dominant mechanism of atom loss from a trap is due to collisions with room-temperature background gas. Before the start of this project, very little was known about the details of background gas collisions on *cold*, trapped atoms as previous studies had mostly focussed on background gas collisions with room-temperature atomic samples. This project therefore made an extensive study of background gas collisions with cold atoms

[Cybulski2019] and found not only the loss rate of atoms from the trap as a function of vacuum pressure, but also the size of collisional frequency shifts.

For neutral atoms trapped in an optical lattice, atomic decoherence can arise from the scattering of lattice photons. This effect was investigated in neutral Sr and the scattering rate was compared to that of spontaneous decay out of the clock's upper state, which was also measured for the first time in this project [Dörscher2018]. It was found that at typical lattice depths, decoherence due to lattice photon scattering dominates over the spontaneous decay rate from the clock's upper state, but neither of these effects prevents probing the atoms coherently on timescales ~ 1 s.

For single-ion clocks, motional heating of the ion can lead to dephasing of the atomic interactions with the probe light. This can limit the maximum useful probe time and hence the achievable linewidth and stability of the clock. New ion traps were developed within this project, and a new state-of-the-art was achieved in the motional heating rate of single ions in an end-cap style trap.

More details from the investigations into effects that can limit the maximum probe time are presented below.

Atom loss from background collisions

When a hot atom from a room-temperature background gas collides with a cold, trapped atom, it can knock the atom from the trap so that the cold atom no longer contributes to the clock signal. By measuring the lifetime of trapped Sr atoms as a function of the background gas pressure, it was found that loss from the trap was at a rate of $0.43(10) \times 10^9$ s^{-1}/mbar. Typical background pressures of 10^{-10} mbar therefore support a Sr atom lifetime in the trap of around 23 s, which is easily long enough to support > 1 s probe times.

However, if the collision with the background gas does not contain enough energy to knock the atom completely out of the trap, then the cold atom will remain and give rise to a frequency shift in the clock signal. Theoretical investigations were carried out to estimate the size of this frequency shift in Sr and Yb. If large enough, collisional shifts could lead to a frequency broadening of the atomic clock transition and limit the maximum probe time, and hence stability, of the clock.

Collisions between trapped atoms and background gases are governed by long-range interactions, which can be approximated by the Van der Waals potential. The collisional shifts can therefore be estimated from knowledge of the coefficient, C_6, which characterises the strength of the interaction potential. In optical atomic clocks, the background gas composition is mostly hot clock atoms that have not been trapped, and molecular hydrogen coming out from the walls of the vacuum system. It was therefore necessary to establish the C_6 coefficients for interactions between the cold clock atoms with both hydrogen and hot clock atoms [Cybulski2019]. The results derived from theory developed in this project for neutral Sr and Yb are shown in the table below.

Table 1: Theoretical results for C_6 parameters and corresponding ratio of fractional frequency shifts / losses caused by background collisions

System	Maximum C_6 [a.u.]	Theory ($\Delta\nu_{bg}$ / ν_0 Γ_{bg}) [s]
Yb (cold) – Yb (hot)	-2561(95)	$-1.09(14) \times 10^{-17}$
Yb (cold) – H_2 (hot)	-217(22)	$-1.46(43) \times 10^{-17}$
Sr (cold) – Sr (hot)	-4013(50)	$-1.1369(54) \times 10^{-17}$
Sr (cold) – H_2 (hot)	-1044(110)	$-1.17(61) \times 10^{-17}$

The results are quoted as a ratio of fractional frequency shift ($\Delta\nu_{bg}$ / ν_0) to collisional loss rate (Γ_{bg}) in order to allow the numbers to be readily applied to experiments. For example, if the measured trap lifetime ~ 10 s, then Γ_{bg} ~ 0.1 s^{-1} which will result in a fractional frequency shift ~ (0.1 s^{-1}) × (-1 × 10^{-17} s) ~ -1 × 10^{-18}. It can

therefore be seen that collisions between cold trapped atoms and the background gas do not result in frequency shifts large enough to cause appreciable broadening of the clock transition at vacuum pressures that are typically achieved in high-accuracy optical clocks. The collisional shifts do not therefore limit the probe time or clock stability, but must be included in the frequency offsets when evaluating the unperturbed clock frequency.

Atomic decoherence

Another effect that can limit the probe interaction time with neutral atoms trapped in an optical lattice is the scattering of lattice photons. This can lead to off-resonant excitation and subsequent spontaneous decay of the atom's internal energy states, causing decoherence of the clock state superposition during the probing. As will be seen below, at typical lattice depths the decoherence rate from lattice photon scattering exceeds that from natural decay out of the upper clock state, and therefore impacts upon the maximum possible probe time and thus the achievable clock stability.

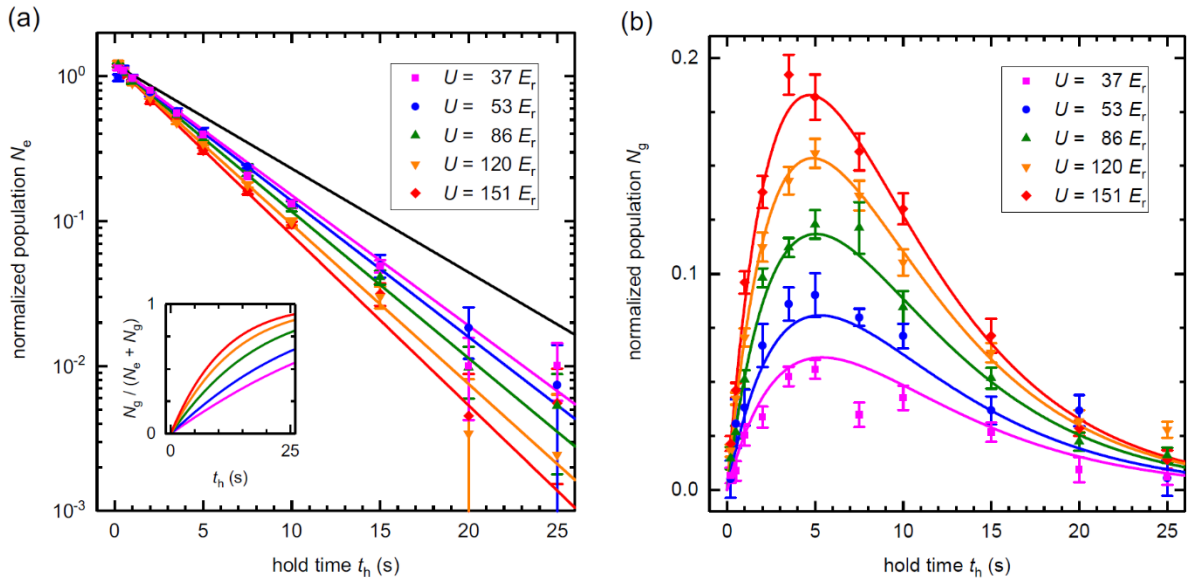

Figure 4: Measured populations in (a) the metastable states $^3P_{0,2}$ and (b) in the ground state $^1S_0$ for samples prepared in the excited state at different lattice depths U as a function of hold time t_h. Results of a combined fit of a rate equation model are shown. Graphs reproduced from [Dörscher2018].

Experimental measurements were made to establish the rate at which ^{87}Sr atoms decay from the excited state $^3P_0$ into the ground state $^1S_0$ due to scattering of lattice photons [Dörscher2018]. The atoms were prepared initially in the excited state and held for varying times, t_h before measuring the populations in the ground and excited states. The experiment was repeated with different lattice depths and the results are shown in Figure 4. The decay out of the excited state and back towards the ground state is clearly visible, with the population in the ground state becoming substantial after several seconds in deep lattice potentials.

In this project, the rate coefficient of decay from $^3P_0$ to $^1S_0$ due to lattice photon scattering was determined to be $\Gamma_L = (556 \pm 15) \times 10^{-6}$ s^{-1} / E_r, where E_r is the lattice photon recoil energy. The spontaneous decay rate of the $^3P_0$ state in ^{87}Sr was also deduced for the first time in this project and found to be $\Gamma_s = (3.0 \pm 1.3) \times 10^{-3}$ s^{-1}. We can therefore see that for all lattice depths above 5 E_r, the decoherence effect of lattice scattering exceeds that of spontaneous decay, and limits the useful probe interrogation time to the order of 100 s. At typical lattice depths of 50 - 100 E_r, the useful interrogation time then becomes ~ 10 s, which still exceeds the 1 s target in this project, but must not be ignored as laser coherence times improve beyond this in the future.

Dephasing of the atomic interactions

Lattice photon scattering is not a concern for single-ion clocks as the ions are trapped in radiofrequency electric fields rather than optical potentials. The dominant problem for single-ion clocks, however, is that of motional heating. As the ion heats, its quantum mechanical wavefunction is spread over an increasing number of

energy levels within the trap. This results in a larger spread of atom-light coupling strengths, which in turn leads to a dephasing or 'washing out', of the coherent interactions with the probe light. To achieve interaction times with the probe light of ~ 1 s, the motional heating should not exceed ~ 10 energy levels, or motional quanta, of the trap per second.

Motional heating can be caused by voltage noise from external sources, but it can also be caused by less-well-understood electrode surface noise. To our knowledge, at the start of this project, the only other ion traps that had demonstrated motional heating rates below 10 quanta s^{-1} were all based on a linear geometry of the trapping electrodes, suitable for trapping arrays of ions. For single-ion clocks, a different geometry is required such as an end-cap style of Paul trap. The trap geometry is significant because empirical evidence suggests that electrode surface noise depends on the distance of the ion from the electrodes as well as on the choice of materials and surface roughness of the electrodes.

Four different designs of end-cap trap were developed in this project and a photo from each is shown in Figure 5. As can be seen, they all share a common geometry with conical electrodes (towards the centre in each picture) providing the dc voltages, and with the radiofrequency electrodes along the axis of the cones.

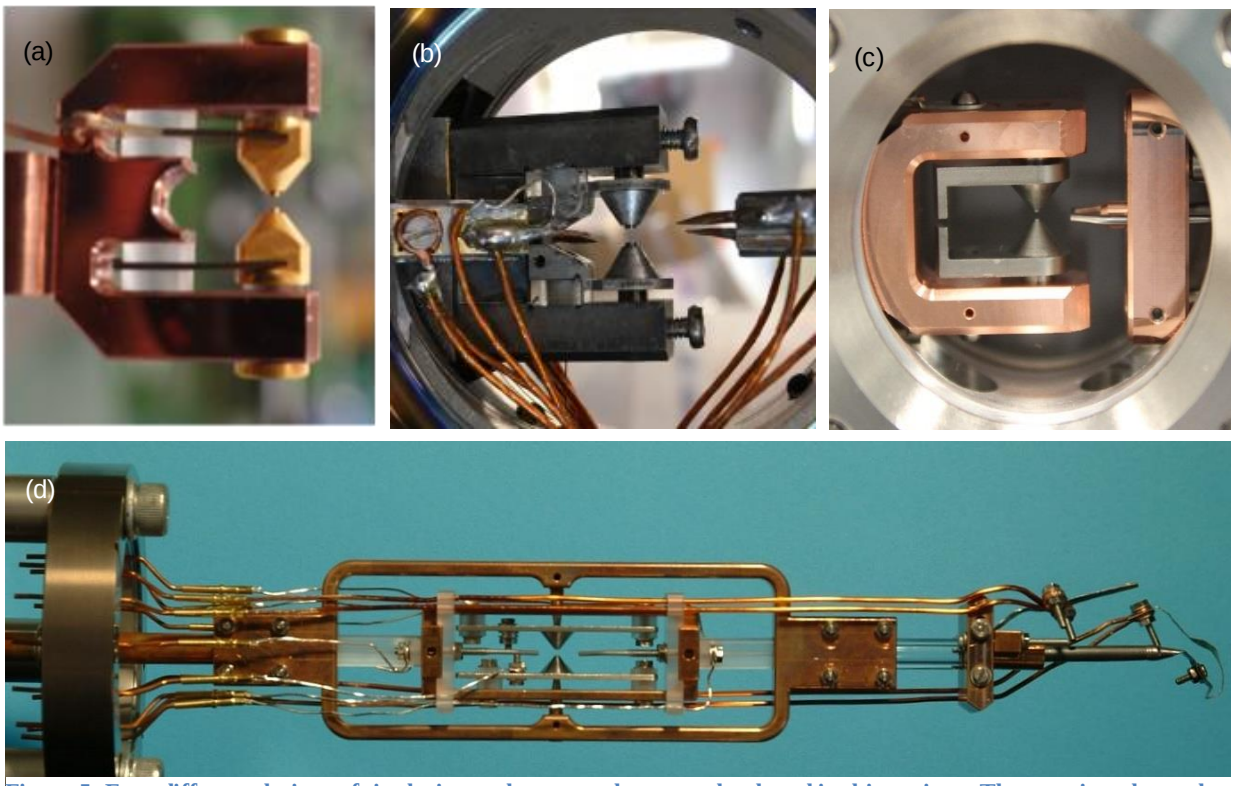

Figure 5: Four different designs of single-ion end-cap trap that were developed in this project. The trapping electrodes were all based on a similar geometry but differed in the choice of materials and surface preparations.

A key difference between the traps was the choice of materials and surface preparations. It is desirable to have a smooth surface on the trapping electrodes facing the ion. In some cases, molybdenum was used as this is a very hard material that can be highly polished; in other cases, the electrodes were evenly sputtered with gold. The 'C'-shaped structure supporting the electrodes was made from either copper or molybdenum, with the main consideration being good thermal conductivity to ensure any heat generated near the ion could be conducted away. Due to manufacturing delays, particularly with parts made from molybdenum, which is a very difficult material to machine, not all the traps were fully characterised before the end of the project. Nevertheless, the trap shown in Figure 5(a), with gold-sputtered molybdenum electrodes, was found to exhibit a heating rate of just 3.6 quanta s^{-1}, compatible with coherent probe times > 1 s.

Conclusion for Objective 2

The key results from this objective have therefore been:

(a) By working with currently achievable vacuum pressures ~ 10^{-10} mbar, background gas collisions do not limit coherent interaction times with neutral Sr atoms up to ~ 10 s, but they can lead to 10^{-18} level frequency offsets.

(b) For neutral Sr atoms trapped in optical lattices with depths of 50–100 E_r, decoherence due to lattice photon scattering dominates over the spontaneous decay rate from the clock's upper state, but neither of these effects limits coherent probing on timescales ~ 1 s.

(c) For single ions trapped in an end-cap trap, motional heating rates of 3.6 quanta s^{-1} have been demonstrated, which are compatible with coherent probe times > 1 s.

The traps that have been developed for single ions and neutral atoms have therefore been shown to support > 1 s probe times, thus achieving the target in Objective 2. Guidelines were written for optimising ion trap design and a report was written to summarise the results of decoherence effects in neutral atom systems.

With the ultrastable lasers from Objective 1 providing a low-noise optical frequency source, and the traps from Objective 2 supporting coherent probing, it was then possible to demonstrate the spectroscopic resolution that could be achieved with a 1 s probe time. Figure 6 shows the result of probing a single ion of $^{171}Yb^+$ around its clock transition at 467 nm with a Rabi pulse of duration 1 s. The full-width-half-maximum frequency is very close to the theoretical Fourier limit of 0.8 Hz, creating a world-leading linewidth for single ions in end-cap style traps.

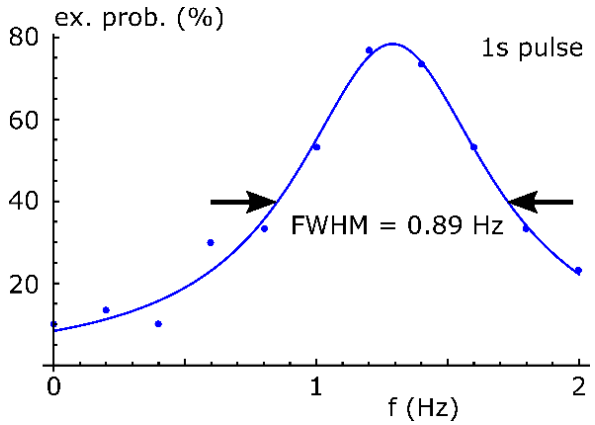

Figure 6: Spectroscopic signal achieved with probing $^{171}Yb^+$ in an end-cap trap with a 1 s Rabi pulse from the clock laser.

4.3 Objective 3 - Evaluating and reducing systematic uncertainties

All sources of systematic frequency shifts that can affect optical clocks need to be well understood and controlled to achieve fractional frequency uncertainties down to the level of 1×10^{-18}. At the beginning of the project, the dominant frequency uncertainties were identified to come from: (i) blackbody radiation (BBR) shifts from the atoms' thermal environment, (ii) light shifts from the optical lattice in neutral atom clocks and (iii) collisional shifts resulting from the collisions between atoms trapped in a lattice. Understanding these three frequency shifts and reducing their contributions to the uncertainty budget of the clocks therefore formed the focus of Objective 3.

For the blackbody radiation shift, the project results demonstrated that sufficient control could be gained over the thermal environment to contribute no more than 10^{-18} to the fractional frequency uncertainties for both neutral atom and single-ion clocks. Techniques included a room-temperature vacuum chamber with thermal shielding which was a first for Europe, and a new cryogenic system that supports blackbody radiation shift uncertainties of just a few parts in 10^{19}. Designs were assisted by finite element modelling and characterisation of material emissivities, and the experimental measurements on the resulting systems showed excellent agreement with the finite element models.

Studies of lattice light shifts and collisional shifts revealed that these effects could also be controlled with fractional frequency uncertainties at the 10^{-18} level. Experimental studies in both Sr and Yb clocks showed that this uncertainty could be achieved even for moderate trap depths. The theory associated with the collisional shifts led to two orders of magnitude improvement in the uncertainty of s-wave scattering lengths for Yb atoms [Borkowski2018a], and has also resulted in a novel proposal for a lattice clock based on weakly bound molecules [Borkowski2018b].

Blackbody radiation (BBR) shift

The BBR shift is the leading term in the uncertainty budget for many optical clocks and is the shift that received the most attention in this project. Contributions to the BBR shift uncertainty arise from both the uncertainty in the atomic response to the radiation (characterised by the differential polarisability coefficient) and uncertainty in the thermal field at the position of the atoms. Before the start of this project, several groups had reported high-accuracy measurements of the polarisabilities for different atoms. What remained for this project, therefore, was to develop sufficient control over the thermal environment for both room-temperature and cryogenic clocks to be able to reach 10^{-18} uncertainties.

In neutral atom clocks, the thermal environment experienced by the atoms is governed largely by the vacuum chamber. In this project, two different vacuum chambers for optical lattice clocks were designed and tested: one for atoms at room-temperature and the other for a cryogenically cooled system. In both cases, the resulting thermal uniformity was assessed with several calibrated thermometers spread across the thermal shields.

The room-temperature design was made with two separated and nested vacuum chambers. The inner chamber was a BBR shield, which also maintained the ultra-high-vacuum necessary for atomic manipulation. The outer chamber maintained a high vacuum, ensuring that the inner BBR shield had a layer of thermal isolation from the external environment. This is the first adoption of this approach in Europe. The BBR shield, shown in Figure 7, was made of copper and coated on the inside with a high-emissivity carbon-nanotube material to reduce stray BBR reflections. The high thermal conductivity of copper and its isolation under vacuum achieved high thermal uniformity with gradients < 45 mK across the entire chamber. This is suitable for reaching a BBR fractional frequency shift uncertainty of 9×10^{-19} with ytterbium. Moreover, this chamber will also be suitable for applying high-voltage fields to measure any dc Stark shifts that may also be present.

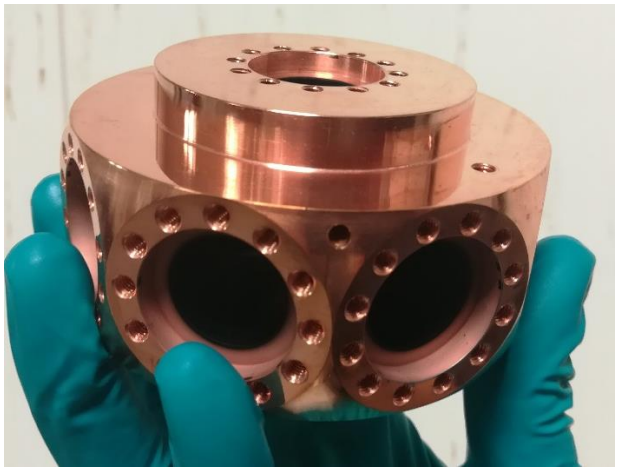

Figure 7: A photograph of the BBR shield used to achieve high thermal uniformity, with gradients < 45 mK, in a room-temperature setup.

The cryogenic vacuum chamber in this project was designed to work at temperatures below 80 K and features an inner copper shield, cooled by a closed-cycle pulse-tube cooler. The novel feature of this design is that it does not require atom translation from a loading region to a science region, but atoms are loaded directly into the science region. This avoids degrading the duty-cycle, and thus stability, of the clock. Temperature gradients on the shield were measured to be < 40 mK corresponding to BBR shifts in strontium with an uncertainty of just a few parts in 10^{20}. Leakage of external blackbody radiation through the viewports and

aperture must be taken into account but, even so, a BBR shift uncertainty of a few parts in 10^{19} is achievable, which represents a new state-of-the-art.

Ion clocks generally exhibit smaller BBR shifts than neutral atom clocks, so do not require special thermal shields. Nevertheless, a careful determination of the thermal environment is still necessary. Temperature sensors such as thermistors, however, are perturbed by the radio-frequency fields used in ion traps. This project therefore investigated the possibility of integrating fibre GaAs temperature sensors into ion traps, with the hope of providing a permanent readout of the temperature close to the ion. Unfortunately, these sensors showed reproducibility issues originating from the losses at the vacuum chamber feedthrough, so were not suitable for integrating inside ion traps. They were, however, found to be insensitive to radio-frequency field and could therefore be used outside the vacuum chamber, around the helical resonator and radio-frequency feedthrough, where the heating currently dominates ion trap temperature rises. GaAs bandgap thermometers with free-space readout were also considered but they had an accuracy and stability worse than the commercial fibre-coupled devices.

To avoid attaching temperature sensors to the trap structure, thermal imaging can also be used to determine the effective temperature in ion traps. Imaging can be performed in operational traps, but the vacuum chamber windows must have suitable transmission for the infrared wavelengths detected in thermal cameras. A further complication with thermal imaging of ion traps is that many of the surfaces are metallic and shiny, with low emissivity. It was therefore necessary to prepare special high-emissivity regions, such as by introducing black patches onto the surfaces, in order to get better accuracy temperature readings. In this project, the two traps shown in Figure 5(c) and (d) were characterised by thermal imaging. It was found that the heating in the Figure 5(c) trap was dominated by the helical resonator, but this could be minimised by forced cooling (air or water) or by a new resonator design.

Finite Element Modelling (FEM) was also used to study the thermal properties of the environment as seen by the atom. FEM can be used to investigate both the heat generation in the physics package (e.g., from radiofrequency resonators and feedthroughs) and the blackbody radiation as seen by the atom (usually modelled as a small perfect blackbody sphere). As an example, Figure 8 shows the results of the temperature modelling for all the different components of the ion trap in Figure 5(d). In this project, FEM was carried out for the two ion traps shown in Figure 5(c) and (d), as well as the two new vacuum chambers for optical lattice clocks. The FEM calculations agreed well with the measurements that were carried out and assisted in the design choices. All four systems were demonstrated to have small enough temperature uncertainties to achieve 10^{-18} level uncertainties or below in the BBR shift.

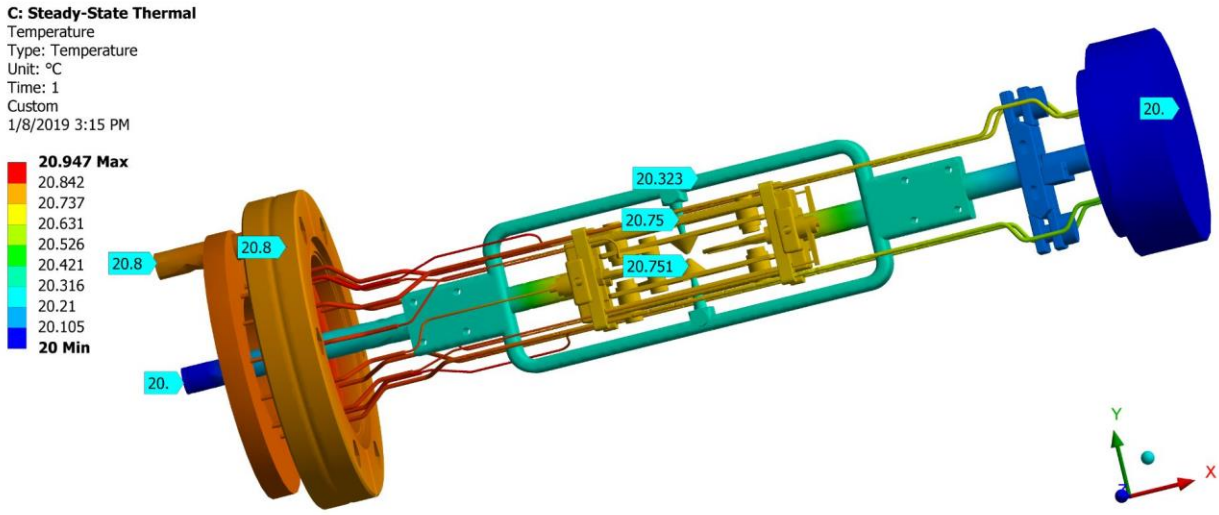

Figure 8: Results of finite element modelling carried out to assess the temperature of all the components in the ion trap pictured in Figure 5(d).

To be able to convert between measured temperature rises and the thermal radiation experienced by the atoms, it is important to have good knowledge of the emissivities of the materials involved. This is far from straightforward as the emissivities may depend on temperature, roughness and surface finish or on the state of oxidation. Two strategies to measure surface emissivities were pursued during this project. One method used the thermal imaging techniques developed for ion traps to measure the radiation emitted from titanium,

molybdenum, copper and fused silica with respect to a black aluminium reference surface. The second method was a more innovative approach that avoided the limits imposed on spectral coverage by thermal cameras, and enabled the total emissivity across the whole BBR spectrum to be measured. It involved placing the test sample in a specially designed vacuum chamber, shown in Figure 9, immersed in a water bath for temperature uniformity. A peltier module was used to heat the sample to a known temperature, which was recorded via a thermistor in the sample (shown with a green connection in the schematic). The blackbody radiation emitted from the sample, which depends on the emissivity coefficient, was then picked up on a thermometer plate opposite, and the resulting temperature rise was recorded by a thermistor in the thermometer plate (shown with a red connection in the schematic). The chamber featured a simple geometry for easy calculations: the diameter to separation ratio of the two plates was around 50 and the view factor between the plates was equal to 0.94, giving a good approximation to the ideal case of two infinite plates. The materials investigated included aluminium, stainless steel, titanium, and copper at different temperatures and with different surface finishes.

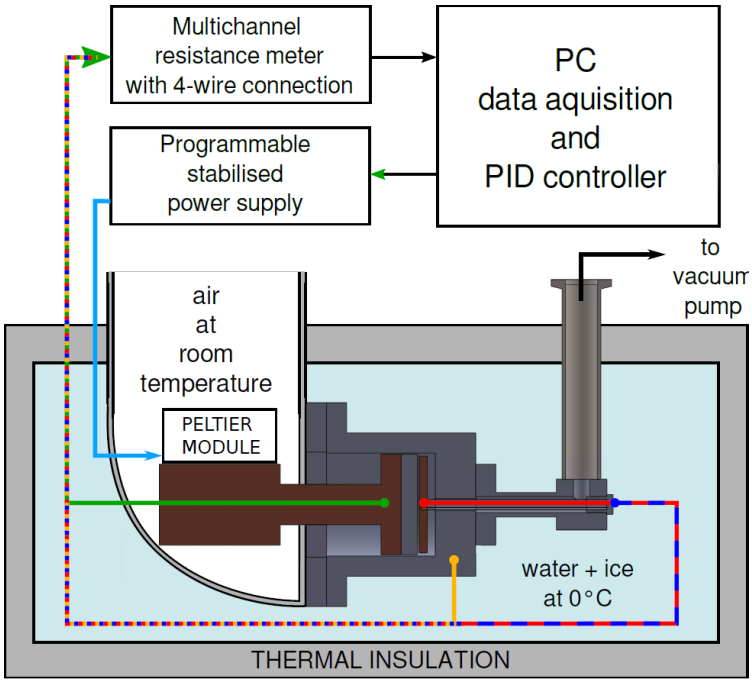

Figure 9: Schematic of an experimental setup to measure emissivity coefficients. The peltier module heats the test sample to a known temperature, recorded by a thermistor in the sample (via the green connection). The blackbody radiation emitted by the sample causes a temperature rise on a thermomenter plate opposite, which is recorded by a thermistor in the thermomenter plate (via the red connection).

Light shifts from optical lattices

In strontium and ytterbium optical lattice clocks, the light shifts from the lattice are the biggest contributions to the uncertainty after the BBR shift. While the linear light shift can be cancelled by tuning the wavelength of the lattice light to the so-called 'magic wavelength', second order shifts arising from atomic hyperpolarisability, multipolar effects and atomic temperatures need to be carefully characterised. Hyperpolarisability is the biggest of these effects and can be investigated directly by observing the frequency shift in different depths of the lattice potential, created by different intensity lasers. Alternatively, it can be investigated indirectly by measuring two-photon transitions near the magic wavelength.

In this project, experiments were conducted to measure the hyperpolarisability of the ^{87}Sr clock transition for different orientations of the polarisation of the trapping light with respect to the atoms' quantisation axis. The hyperpolarisability causes a frequency shift of 0.45(10) μHz/E_r^2, which is a fractional shift of the clock transition of 1×10^{-17} for a trapping depth of 100 recoil energies, with an uncertainty of 1×10^{-18}. Different linear polarisations of the lattice light were used, but it was found that there was no dependence of the hyperpolarisability with the orientation of this polarisation.

Measurements were also carried out of the two-photon resonances near the magic wavelength for ^{171}Yb to constrain the hyperpolarisability coefficient in Yb optical lattice clocks. The measurements predicted a shift of

-2 × 10^{-17} at 100 recoil energies, with an uncertainty of 2 × 10^{-18}. These results are consistent with those also measured by groups in the USA and Japan in the last year, but relied on very different methods, thus giving confidence to the values obtained.

Collisional shifts within optical lattices

Collisions between trapped atoms and background gas atoms were investigated as part of Objective 2. Here, the so-called 'density shifts' arising from collisions between atoms trapped *within* the lattice potential were studied. The magnitude of the shift depends not only on density, but also on whether the atom is a boson or fermion, the purity of spin polarisation of the atomic sample and the fraction of atoms in the excited state. It was found from theoretical investigations in this project that density shifts as large as 10^{-16} could be suppressed by two orders of magnitude by using tailored Ramsey spectroscopy and controlling the excitation fraction to within one percent.

The theoretical investigations relied on determining atomic interactions. The interactions were modelled using an ab initio mass scaled Born-Oppenheimer potential whose long-range parameters were fit to experimental data [Borkowski2018a]. This theory was used to calculate the s-wave scattering lengths for bosonic isotopic pairs of ytterbium atoms (using experimental input from high-resolution two-color photoassociation spectroscopy of Bose-Einstein condensates) with an uncertainty over two orders of magnitude smaller than previous determinations. These studies also yielded a proposal for a novel molecular optical clock [Borkowski2018b].

Conclusion for Objective 3

The key results from this objective have been:

(a) New vacuum chamber designs for a room-temperature ^{171}Yb clock and a cryogenic ^{87}Sr clock that have demonstrated sufficient thermal control to contribute less than 1 × 10^{-18} to the fractional frequency uncertainty of the clocks.

(b) Detailed knowledge of material emissivities and Finite Element Modelling to demonstrate ion traps for $^{171}Yb^{+}$ and $^{88}Sr^{+}$ clocks that also exhibit sufficient thermal control to contribute at the 10^{-18} level to the fractional frequency uncertainty of the clocks.

(c) Control of lattice light shifts at the 10^{-18} level in lattice depths of up to 100 E_r. The hyperpolarisability coefficient was also found to have no dependence on the polarisation direction of the light at this level of uncertainty.

(d) New theory was developed for collisions, showing that uncertainties at the 10^{-18} level are achievable with the operating conditions in optical clocks.

The target uncertainty level of 10^{-18} for all three shifts under investigation in Objective 3 has therefore been met. The project has built up a significant body of knowledge within Europe on how to handle these systematic shifts for existing and future clocks. For example, control of the BBR shift at the 1 × 10^{-18} had previously only been achieved in the USA and Japan. Reports were written, summarising the control and evaluation at the 10^{-18} level of frequency shifts arising from blackbody radiation, lattice light shifts and collisional shifts.

4.4 Objective 4 - Optimised interrogation methods and validation of clock performance

4.4.1 Optimised interrogation methods (Objective 4)

Frequency instability in optical clocks was improved in Objectives 1 and 2 by enabling longer coherent interaction times between the clock laser and trapped atoms. Frequency inaccuracy was improved in Objective 3 by reducing the perturbations from the environment around the atoms. The target in the first part of Objective 4 was to reduce the instability and inaccuracy of the clocks still further, by applying optimised interrogation methods with careful choices of probing sequences and timings.

To establish the optimum probing time in order to minimise clock frequency instability, a theoretical analysis was carried out in this project [Leroux2017]. It was a comprehensive study that took into account different frequency-noise processes that are typically present in laser light. A separate experimental study to reduce

clock frequency instability arising from the Dick effect was also pursued, which saw the first demonstration in Europe of an optical lattice clock being operated with a 50% duty cycle [Vallet2017].

To tackle inaccuracy arising from probe-related effects, a novel sequence of pulses was developed (called autobalanced Ramsey) which provided immunity to a wide variety of probe-pulse induced shifts [Sanner2018 (ABR)]. This method was demonstrated to be so successful at suppressing frequency shifts that it has already been taken up by two independent research groups outside the consortium: one in France and one in the USA, and incorporated into their clock operation.

More details are given below about the different probing techniques that were investigated.

Interrogation methods to reduce instability

The fractional frequency instability is an important performance criterion since it determines the averaging time required for the frequency output from a clock to reach a given uncertainty level. Longer probe times will allow lower frequency instabilities, and thus shorter averaging times, but the maximum useful probe time is generally limited by the coherence length of the laser. To determine the optimum probe time, it is therefore necessary to take account of the nature of the frequency noise in the laser source.

Using simple analytical models and numerical simulations, the optimum probe times were derived in this project as a function of clock atom number, N and of the dominant noise type in the laser source [Leroux2017]. The calculations assumed that there was no dead-time in each probing cycle of the clock and so the Dick effect could be neglected. Furthermore, spontaneous emission from the excited clock state was also neglected. The different noise types considered were white frequency noise, flicker frequency noise and random walk. The optimum interrogation times, T were evaluated for Ramsey spectroscopy and are shown in Table 2. The times are scaled relative to a characteristic time, Z which satisfies $\sigma_L(Z) = 1/\omega Z$, where $\sigma_L(Z)$ is the Allan deviation of the laser frequency noise, and ω is the angular frequency of the clock transition. In other words, Z is the choice of probe time for which the Allan deviation of the laser noise at one clock cycle is as large as the quantum projection noise of a single atom. For typical optical frequency standards with a fractional laser instability around 10^{-16}, Z will therefore be on the order of a few seconds.

Table 2: Recommendations for the choice of Ramsey interrogation time. The last column gives the optimal probe time in the limit of many atoms. There is nothing to be gained by probing longer than this time. It may be necessary to use shorter probe times to avoid fringe hops; a suggested safe upper bound on the probe time is given in the second column. Table reproduced from [Leroux2017].

Laser noise type	Safe T / Z	Asymptotic optimum T / Z
White frequency	-	$\min(N^{-1/5}, 1.4\ N^{-1/3})$
Flicker frequency	$0.4 - 0.15\ N^{-1/3}$	$0.76\ N^{-1/6}$
Random walk	$0.4 - 0.25\ N^{-1/3}$	$0.79\ N^{-1/9}$

The assumption that there is no dead-time in each probing cycle of the clock is often reasonable for ion optical clocks, where the ion is trapped and used repeatedly from one probe cycle to the next. For neutral atom clocks, however, the atom cloud is generally lost after each probing cycle and must be reloaded into the lattice trap. This introduces dead-time, during which the laser noise is not being sampled by the atoms. There can then be an aliasing effect (known as the Dick effect) in which high frequency noise on the laser is converted into undesirable noise at the frequency of the clock cycle. This effect becomes more pronounced with increasing dead-time and generally limits the achievable frequency instability of neutral atom lattice clocks.

To avoid dead-time in the clock cycle, one approach is to run two clocks, each with 50% duty cycle, in an interleaved manner. This ensures the laser is continuously sampled and eliminates the Dick effect. The experimental realisation of a 50% duty cycle, however, is not straightforward as the time to reload the atoms must be shorter than the probe time. One approach is to extend the probe time, using a laser with a very long

coherence time. But this defeats the point of an interleaved clock, whose advantage is precisely to enable very low instabilities without resorting to advanced laser stabilisation techniques.

In this project, a different approach was taken, by designing a pulse sequence for a ^{87}Sr clock that took advantage of cavity-assisted non-destructive detection of atoms [Vallet2017]. The exquisite signal-to-noise ratio of this detection, capable of resolving just a few atoms in the optical lattice, made it possible to operate the clock with a reduced number of atoms (a few hundred) without being limited by the detection noise. With this feature, a workable short clock sequence was demonstrated with a duration of 400 ms and a 50% duty cycle, which avoids the need for state-of-the-art laser coherence times. Furthermore, this detection also makes it possible to reuse the atoms from one cycle to the next, thus offering the possibility of further reducing the clock dead-time.

Interrogation methods to reduce inaccuracy from probe-related shifts

The desired output frequency of an atomic clock is that of the *unperturbed* atomic transition. It is inevitable, however, that probing the atom will disturb the very transition that is being used as the reference. For many optical clocks, the intensity of the probe beam is sufficiently weak that the resulting disturbances lead to fractional frequency shifts well below the 10^{-18} level, so can be neglected. There are notable exceptions, however, for which a much more intense probe beam must be used to drive the clock transition. These include the $^1S_0 \rightarrow {}^3P_0$ transitions in bosonic optical lattice clocks (e.g. ^{88}Sr, ^{174}Yb, ^{24}Mg) and the electric octupole transition in the $^{171}Yb^+$ single-ion clock. With a more intense probe beam, ac Stark shifts induce a frequency offset that must be carefully compensated, otherwise inaccuracies in the resulting clock frequency may be significantly above the 10^{-18} level.

The simplest way to remove frequency offsets caused by the intensity of the probe beam is to measure the clock frequency when probed with two different intensities, and then to extrapolate to the unperturbed frequency. Whilst conceptually simple, this method requires extreme control over the stability of the powers at the two different levels and the electronics used to monitor those power levels must be carefully designed. As an alternative to the extrapolation technique, a novel probing scheme was also designed in this project, employing a tailored sequence of pulses called 'autobalanced Ramsey'. It works on the principle of interleaving two Ramsey sequences with different free evolution periods, and servoing the laser frequency or phase so that the two sequences produce identical excited state populations [Sanner2018]. This indicates that the longer Ramsey dark time does not result in an additional phase difference between the laser and the atoms, i.e. that the laser is in resonance with the unperturbed atomic frequency.

Both techniques allowed the $^{171}Yb^+$ electric octupole clock to enter the 10^{-18} level of inaccuracy, suppressing shifts of up to several 100 Hz to the mHz level. However, the latter also had the advantage of tolerating errors in the interrogating pulses (such as optical phase chirps or transient Zeeman shifts) provided they were consistent with neighbouring short evolution-time interrogations. The autobalanced Ramsey sequence also demonstrated improved frequency instability over the extrapolation technique as it introduced less temporal overhead into the clock cycle.

4.4.2 Validation of clock performance (Objective 4)

For the majority of the project, the emphasis had been on improving the performance of the optical clocks in Europe. At the end, it was then important to assess the fractional frequency uncertainties that were achieved, and this was the focus in the second part of Objective 4. The performance was judged in three different ways: (i) estimated uncertainty budgets for individual clocks, (ii) frequency comparisons between pairs of clocks of the same type and (iii) comparisons of the frequency ratio between pairs of clocks of different types.

The estimated uncertainty budgets for the optical lattice clocks and single-ion clocks revealed significant improvements since the start of the project with half of the clocks that were characterised showing at least a factor of 4 improvement in their accuracy. A frequency comparison between two Yb^+ clocks was used to validate their estimated uncertainty budgets, and also exhibited world-leading agreement between a pair of ion optical clocks, with the results published in Nature [Sanner2019]. Excellent agreement was also found in a comparison of the Yb^+/Sr frequency ratio which was measured at two different institutes. Such ratios allow the performance of clocks in different institutions to be assessed, without a direct link between the institutions.

The sections below give more details from each of these measurement approaches to validate the performance of the clocks in this project.

Estimated uncertainty budgets

Nine different clocks were assessed by estimating their uncertainty budgets. This involves taking account of all the different effects that could lead to a frequency offset (electric fields, magnetic fields, atomic motion etc.) and assessing in turn the magnitude and uncertainty of each shift. Adding all the effects together gives an indication of the frequency correction that should be applied to the output of the clock, and the associated uncertainty is a prediction of the clock's inaccuracy.

The three ion clocks ($^{171}Yb^+$) that were assessed in this project all reached uncertainties in the 10^{-18} range. The full uncertainty budget that has been published for two of these clocks is given in Table 3, showing the total uncertainties to be 2.7×10^{-18} and 3.0×10^{-18}. For the six optical lattice clocks that were evaluated (^{87}Sr, ^{88}Sr, ^{171}Yb), significant contributions to the uncertainty budget in each case came from the blackbody radiation and lattice light shifts, at the level of about 1×10^{-17}. The new vacuum chamber designs and lattice light shift corrections, developed for Objective 3, have demonstrated that they can significantly reduce these contributions to the 1×10^{-18} level or below, so the lattice clock uncertainties should also be in the 10^{-18} range once these new designs are incorporated into the operational clocks.

Table 3: Systematic frequency shifts, $\Delta\nu_{1,2}$ for Yb^+ clocks 1 and 2 and their corresponding uncertainties given as fractions of the unperturbed E3 transition frequency ν_0. The final column gives the expected frequency difference (and corresponding uncertainty) between clocks 1 and 2. Table reproduced from [Sanner2019].

Shift effect	$\Delta\nu_1/\nu_0$ (10^{-18})	$\Delta\nu_2/\nu_0$ (10^{-18})	$\Delta\nu_{1-2}/\nu_0$ (10^{-18})
Second-order Doppler	-2.3 (1.5)	-4.0 (2.2)	1.7 (2.7)
Blackbody radiation	-70.5 (1.8)	-69.9 (1.7)	-0.6 (1.7)
Probe light	0 (0.8)	0 (0.5)	0 (0.9)
Second-order Zeeman	-10.4 (0.2)	-11.3 (0.4)	0.9 (0.4)
Quadratic dc Stark	-0.8 (0.6)	-1.3 (0.8)	0.5 (1.0)
Quadrupole	-5.7 (0.5)	-3.9 (0.5)	-1.8 (0.7)
Background gas	0 (0.5)	0 (0.5)	0 (0.7)
Servo	0 (0.2)	0 (0.1)	0 (0.1)
Gravitation	-0.5 (0.1)	0	-0.5 (0.1)
Total	-90.2 (2.7)	-90.4 (3.0)	0.2 (3.6)

Frequency comparisons between clocks

In the absence of any reference frequency to compare a clock against, an estimated uncertainty budget is the best that can be done to determine a clock's inaccuracy. However, it is always possible that there are further effects that shift the clock frequency, which have not been taken into account. In order to validate the uncertainty budget, a comparison between two independent clocks should always be carried out where possible.

The two Yb^+ clocks, whose estimated uncertainties are shown in Table 3, were compared against each other for several months. The frequency difference that was measured between the two is plotted in Figure 10 and was found to be 1.8(2.7) mHz, corresponding to $2.8(4.2) \times 10^{-18}$ in fractional frequency units. The frequency difference was therefore consistent with zero, to within the combined uncertainty of 4.2×10^{-18}. The result is not only consistent with the estimated uncertainty budgets of the two clocks, but is also world-leading: never before have two ion clocks been demonstrated to agree with such a small uncertainty. Further details of this clock-clock comparison are given in the Nature publication, [Sanner2019].

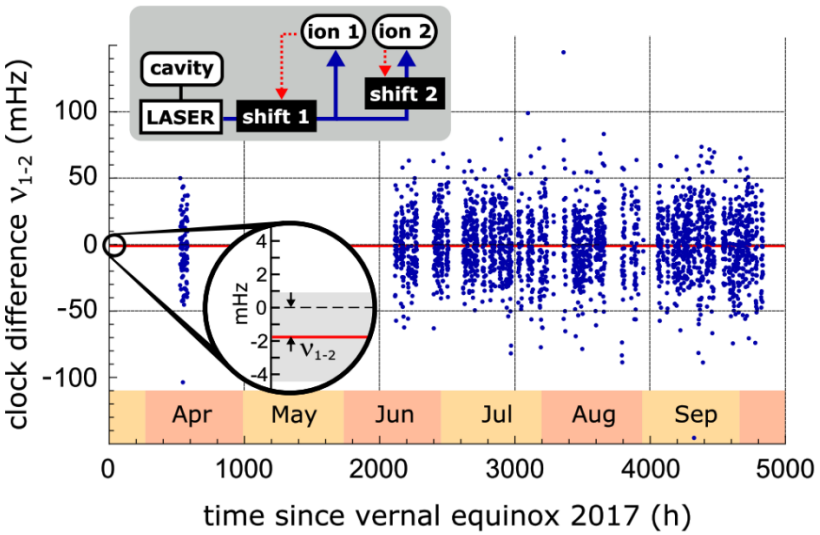

Figure 10: Frequency difference between two Yb^+ ion clocks. Each of the blue data points shows the mean frequency difference from half an hour of data averaging. The red line gives the mean frequency difference from the whole campaign. The magnified region shows the clock difference of 1.8(2.7) mHz, corresponding to 2.8(4.2) × 10^{-18} in fractional frequency units. The inset illustrates the chained configuration of the two clocks. Figure reproduced from [Sanner2019].

Frequency comparisons between a pair of independent clocks can also be used to demonstrate the achieved level of instability. In this project, frequency instability was assessed for six pairs of clocks, including optical lattice clocks and single-ion clocks. The systems showed stability improvements during the course of the project, due largely to the achievements in Objectives 1 and 2. The single-ion clocks reached an instability of $1 \times 10^{-15}/\sqrt{\tau}$. In general, optical lattice clocks exhibit better frequency instability due to the larger number of atoms that are probed in each clock cycle. However, dead-time in the clock cycle results in further degradation of the stability due to the Dick effect. For asynchronous probing of the two clocks (which includes the undesirable Dick effect), comparisons between Sr lattice clocks averaged down as $4 \times 10^{-16}/\sqrt{\tau}$, as shown in Figure 11. Assuming each clock contributes equally to the instability, then the relative instability for each clock is just below $3 \times 10^{-16}/\sqrt{\tau}$.

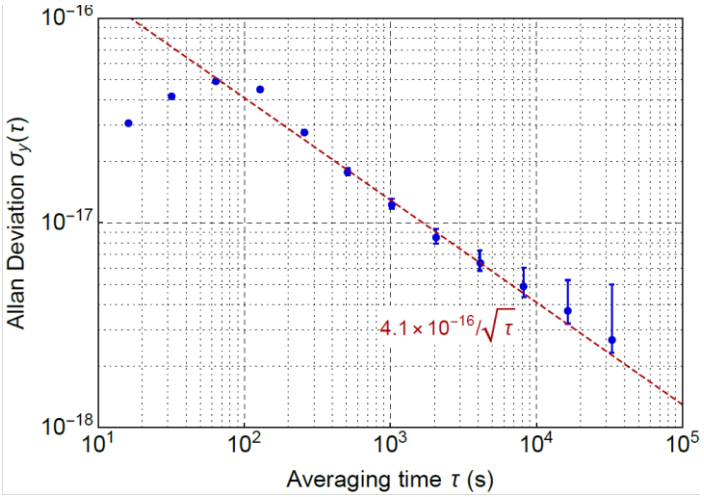

Figure 11: Fractional frequency instability from a comparison between a ^{87}Sr and a ^{88}Sr optical lattice clock. Figure reproduced from [PRA 98, 053443 (2018)].

Comparison of frequency ratios between different clocks

A frequency comparison between two clocks in different institutions gives an even better validation of the clocks' performance since the environmental conditions and experimental designs will generally have far less in common than between two clocks on the same site. It was beyond the scope of this project to operate any links between remote clocks as that was the focus of EMPIR project 15SIB05 OFTEN. Nevertheless, two different consortium partners each had Yb^+ and Sr clocks, so were each able to measure the Yb^+/Sr frequency

ratio. Agreement of the ratios within the predicted uncertainty is then indicative of all four clocks operating at the expected level.

The Yb^+/Sr frequency ratios measured by the two partners were found to agree at the level of 3×10^{-17}, with the uncertainty being dominated by measurement statistics. This result is entirely consistent with the clocks operating within their predicted uncertainty budgets, which were 10^{-17} or below for all four systems.

Conclusion for Objective 4

The key results for the first part of Objective 4 were:

(a) theoretical evaluations of the optimum probing time to reduce clock frequency instability,
(b) experimental demonstration of a clock running with 50% duty cycle as a significant step towards running a dead-time-free system with suppressed frequency instability
(c) design and demonstration of a tailored pulse sequence that reduced clock frequency inaccuracies arising from probe-related effects.

These novel interrogation methods have demonstrated reductions in frequency instability and inaccuracy, thus meeting the target of the first part of Objective 4.

The key results for the second part of Objective 4 were

(a) significant improvements in the performance of European optical clocks during the project. All the ion clocks in this project reached estimated uncertainties in the 10^{-18} range, and for lattice clocks the dominant uncertainties were the BBR and lattice shifts, which will in future be reduced to the 10^{-18} level, following the achievements in Objective 3.
(b) two Yb^+ clocks were compared over an extended period and shown to agree at a world-leading level of 4×10^{-18} for ion optical clocks
(c) two Yb^+/Sr frequency ratios measured at different institutions were shown to agree as expected, within the level of measurement uncertainties, giving confidence in the performance of all four frequency standards, without the use of frequency links between the institutions.

These results show multiple examples of clock performance being demonstrated to reach uncertainties in the 10^{-18} range, thus meeting the target for the second part of Objective 4.

5 Impact

Dissemination and engagement

This project has tackled an ambitious programme of research and published 25 papers in peer-reviewed journals including Metrologia, Physical Review Letters and Nature. The work has been included in more than 100 presentations at international conferences as well as in articles for the popular press, and further engagement with the public has taken place at exhibitions and outreach events. Training opportunities specific to this project have included Researcher Mobility Grants totalling 31 months and a School on Optical Clocks in September 2018, which brought together invited speakers and students for a week of lectures, poster sessions, and interesting discussions.

Impact on metrology and relevant standards

This project has improved the performance of optical atomic clocks across Europe in terms of both accuracy and stability, with the most direct impact for the metrology community being on the top-level realisation of the SI second.

The primary frequency standard, upon which the SI second is currently defined, is based on ^{133}Cs. There are also eight optical frequency standards that are accepted as secondary representations of the SI second, and five of them were included in this project: ^{87}Sr, ^{171}Yb, $^{88}Sr^+$, $^{171}Yb^+$(E2) and $^{171}Yb^+$(E3). Improved performance of these clocks therefore leads to smaller uncertainties in the secondary representations of the SI second. Frequency measurements from the clocks are disseminated to a range of standards and technical committees, including the Frequency Standards Working Group of the Consultative Committee for Time and Frequency (CCTF-WGFS) that makes recommendations on updating values for the secondary representations of the SI second. During this project, two new absolute frequency values were measured [Pizzocaro17, Baynham18]

and many more are planned for the new project 18SIB05 ROCIT, benefiting from the reduced uncertainties that have been achieved in this project.

Beyond the improvements to the secondary representations, it is anticipated that the SI second will itself be redefined in the future, based on an optical frequency standard. The knowledge accumulated in this project, along with the validated results of clock performance, will therefore influence the international decision to choose the optimum atomic clock species for a future redefinition of the second.

Impact on the scientific communities

Beyond metrology, this project has also benefited the scientific community, through the introduction of new techniques as well as the ability to carry out fundamental physics with the clocks themselves.

An example of this project introducing new techniques is the 'autobalanced Ramsey' probing scheme that was developed in objective 4 [Sanner2018]. It proved so successful at suppressing frequency shifts induced by probe pulses that it has already been taken up by two independent research groups outside the consortium: one in France and one in the USA.

For fundamental physics, optical clocks operating at the highest precision can test the laws of physics with unprecedented sensitivity. During this project, such experiments have included tests of special relativity with twice the sensitivity ever achieved before [Delva2017], searches for dark matter with several orders of magnitude better resolution [Wcisło 2016, Wcisło2018] and new limits on Lorentz symmetry violation parameters that improve on previous limits by two orders of magnitude [Sanner2019].

Impact on industrial and other user communities

Objectives 1 and 2 improved clock stability, thus reducing the averaging time needed to reach a given statistical uncertainty. This makes optical clocks more practical for 'in the field' measurements. Examples of end users we have been working with that could benefit from low uncertainty optical clocks include radio astronomers needing to synchronise arrays of telescopes in very long baseline interferometry [Krehlik2017], and surveyors needing high spatial and temporal resolution of gravity potentials [Mehlstäubler2018].

To facilitate end users building up new systems, this project has created a set of practical guidelines, detailing the technical requirements for developing optical clocks with 1×10^{-18} uncertainty. It has drawn on the collective knowledge gained across the objectives and is complementary to reviews of scientific advances that are already available in the published literature. The guidelines have been made publicly available on the arXiv (https://arxiv.org/abs/1906.11495) and the project webpage and will be submitted to EURAMET TC-TF for consideration as a Technical Guide.

The consortium has also been working with industrial organisations in a high-profile project ('Opticlock' - separately funded) to build a demonstrator optical clock, based on single trapped ions, with a view to commercialisation. One of the ion traps designed in objective 2 of this project has demonstrated excellent properties and the Opticlock project will now adopt this ion trap in its systems, thus providing a route for its uptake and exploitation into the commercial market.

Longer-term economic, social and environmental impacts

Precision frequency and timing information is at the core of many technologies upon which society increasingly relies. For example, global navigation satellite systems depend on a constellation of highly precise atomic clocks to provide accurate position and timing information. Improvements in clock performance could therefore enable better navigation in the future. Similarly, better timing signals at the heart of telecommunications systems could result in increased network resilience and lower operating costs; synchronised monitoring of weaknesses in energy networks could enable power to be transferred more efficiently. Improved atomic clocks are therefore likely to bring significant benefits, not just to the level of these services but also by stimulating growth in new applications across a broad range of industries.

In the longer term, the high spatial and temporal resolution of gravity potentials that can be measured with optical clocks is expected to have a large environmental benefit. Data gathered from optical clocks over long timescales could allow monitoring of seasonal and long-term trends in ice sheet masses, ocean current transport and overall ocean mass changes. Such data provides critical input to the models which are used to study and forecast the effects of climate change.

6 List of publications

[Baynham2018] Absolute frequency measurement of the $^2S_{1/2} \rightarrow {}^2F_{7/2}$ optical clock transition in $^{171}Yb^+$ with an uncertainty of 4×10^{-16} using a frequency link to international atomic time
C.F.A. Baynham, R.M. Godun, J.M. Jones, S.A. King, P.B.R. Nisbet-Jones, F. Baynes, A. Rolland, P.E.G. Baird, K. Bongs, P. Gill and H.S. Margolis,
Journal of Modern Optics ***65****, 221-227 (2018)* https://arxiv.org/pdf/1707.00646.pdf

[Bielska2017] Absolute frequency determination of molecular transition in the Doppler regime at kHz level of accuracy
K. Bielska, S. Wójtewicz, P. Morzyński, P. Ablewski, A. Cygan, M. Bober, J. Domysławska, M. Zawada, R. Ciuryło, P. Masłowski and D. Lisak,
Journal of Quantitative Spectroscopy and Radiative Transfer, ***201****, 156 (2017)* https://arxiv.org/pdf/1705.06639.pdf

[Borkowski2017] Optical Feshbach resonances and ground state molecule production in the RbHg system
M. Borkowski, R. Muñoz Rodriguez, M.B. Kosicki, R. Ciuryło and P.S. Żuchowski,
Physical Review A ***96****, 063411 (2017)* https://arxiv.org/pdf/1708.05403.pdf

[Borkowski2018a] Beyond-Born-Oppenheimer effects in state of the art photoassociation spectroscopy of ytterbium atoms
M. Borkowski, A.A. Buchachenko, R. Ciuryło, P.S. Julienne, H. Yamada, Y. Kikuchi, K. Takahashi, Y. Takasu and Y. Takahashi,
Physical Review A ***96****, 063405 (2018)* https://link.aps.org/accepted/10.1103/PhysRevA.96.063405

[Borkowski2018b] Optical lattice clocks with weakly bound molecules
M. Borkowski,
Physical Review Letters ***120****, 083202 (2018)* https://arxiv.org/pdf/1802.08291.pdf

[Cybulski2019] Ab initio studies of the ground and first excited states of the Sr–H_2 and Yb–H_2 complexes
H. Cybulski,
Journal of Chemical Physics ***150****, 064316 (2019)* https://arxiv.org/pdf/1807.05228.pdf

[Delva2017] Test of Special Relativity Using a Fiber Network of Optical Clocks
P. Delva, J. Lodewyck, S. Bilicki, E. Bookjans, G. Vallet, R. Le Targat, P.-E. Pottie, C. Guerlin, F. Meynadier, C. Le Poncin-Lafitte, O. Lopez, A. Amy-Klein, W.-K. Lee, N. Quintin, C. Lisdat, A. Al-Masoudi, S. Dörscher, C. Grebing, G. Grosche, A. Kuhl, S. Raupach, U. Sterr, I. R. Hill, R. Hobson, W. Bowden, J. Kronjäger, G. Marra, A. Rolland, F. N. Baynes, H. S. Margolis, and P. Gill,
Physical Review Letters ***118****, 221102 (2017)* https://arxiv.org/pdf/1703.04426.pdf

[Didier2019] 946-nm Nd:YAG digital-locked laser at 1.1×10^{-16} in 1 s and transfer-locked to a cryogenic silicon cavity
A. Didier, S. Ignatovich, E. Benkler, M. Okhapkin and T.E. Mehlstäubler,
Optics Letters ***44****, 1781 (2019)* https://arxiv.org/pdf/1902.07012.pdf

[Dörscher2018] Lattice-induced photon scattering in an optical lattice clock
S. Dörscher, R. Schwarz, A. Al-Masoudi, S. Falke, U. Sterr and Chr. Lisdat,
Physical Review A ***97****, 063419 (2018)* https://arxiv.org/pdf/1802.02945.pdf

[Gobron2017] Dispersive heterodyne probing method for laser frequency stabilization based on spectral hole burning in rare-earth doped crystals
O. Gobron, K. Jung, N. Galland, K. Predehl, R. Le Targat, A. Ferrier, P. Goldner, Seidelin, and Y. Le Coq,
Optics Express ***25****, 15539 (2017)* https://doi.org/10.1364/OE.25.015539

[Krehlik2017] Fibre-optic delivery of time and frequency to VLBI station
P. Krehlik, Ł. Buczek, J. Kołodziej, M. Lipiński, Ł. Śliwczyński, J. Nawrocki, P. Nogaś, A. Marecki, E. Pazderski, P. Ablewski, M. Bober, R. Ciuryło, A. Cygan, D. Lisak, P. Masłowski, P. Morzyński, M. Zawada, R. M. Campbell, J.

Pieczerak, A. Binczewski, and K. Turza,
Astronomy and Astrophysics ***603****, A48 (2017)* https://arxiv.org/pdf/1703.09479.pdf

[Leroux2017] On-line estimation of local oscillator noise and optimisation of servo parameters in atomic clocks
I. D. Leroux, N. Scharnhorst, S. Hannig, J. Kramer, L. Pelzer, M. Stepanova and P. O. Schmidt,
Metrologia ***54****, 307 (2017)* https://arxiv.org/pdf/1701.06697.pdf

[Matei2017] 1.5 µm lasers with sub-10 mHz linewidth
D.G. Matei, T. Legero, S. Häfner, C. Grebing, R. Weyrich, W. Zhang, L. Sonderhouse, J.M. Robinson, J. Ye, F. Riehle, and U. Sterr,
Physical Review Letters ***118****, 263202 (2017)* https://arxiv.org/pdf/1702.04669.pdf

[Mehlstäubler2018] Atomic clocks for geodesy
T.E. Mehlstäubler, G. Grosche, Chr. Lisdat, P.O. Schmidt and H. Denker,
Reports on Progress in Physics ***81****, 064401 (2018)* https://arxiv.org/pdf/1803.01585.pdf

[Origlia2018] Towards an optical clock for space: Compact, high-performance optical lattice clock based on bosonic atoms
S. Origlia, M.S. Pramod, S. Schiller, Y. Singh, K. Bongs, R. Schwarz, A. Al-Masoudi, S. Dörscher, S. Herbers, S. Häfner, U. Sterr and Chr. Lisdat
Physical Review A ***98****, 053443 (2018)* https://arxiv.org/pdf/1803.03157.pdf

[Pizzocaro2017] Absolute frequency measurement of the $^{1}S_0 - {}^{3}P_0$ transition of ^{171}Yb
M. Pizzocaro, P. Thoumany, B. Rauf, F. Bregolin, G. Milani, C. Clivati, G. A. Costanzo, F. Levi and D. Calonico,
Metrologia ***54****, 102 (2017)* https://doi.org/10.1088/1681-7575/aa4e62

[Rauf2018] Phase-noise cancellation in polarisation maintaining fibre links
B. Rauf, M.C. Vélez López, P. Thoumany, M. Pizzocaro and D. Calonico
Review of Scientific Instruments ***89****, 033103 (2018)* https://arxiv.org/pdf/1807.10818.pdf

[Sanner2018] Autobalanced Ramsey Spectroscopy
C. Sanner, N. Huntemann, R. Lange, C. Tamm and E. Peik,
Physical Review Letters ***120****, 053602 (2018)* https://arxiv.org/pdf/1707.02630.pdf

[Sanner2019] Optical clock comparison for Lorentz symmetry testing
Chr. Sanner, N. Huntemann, R. Lange, Chr. Tamm, E. Peik, M.S. Safronova and S.G. Porsev
Nature 567, 204 (2019) https://arxiv.org/pdf/1809.10742.pdf

[Schäffer2017] Dynamics of bad-cavity-enhanced interaction with cold Sr atoms for laser stabilization
S.A. Schäffer, B.T.R. Christensen, M.R. Henriksen, and J.W. Thomsen,
Physical Review A ***96****, 013847 (2017)* https://arxiv.org/pdf/1704.08245.pdf

[Senel2018] Tailored design of mode-locking dynamics for low-noise frequency comb generation
Ç. Şenel, R. Hamid, C. Erdoğan, M. Çelik, F.Ő. Ilday,
Physical Review Applied ***10****, 024027 (2018)* https://arxiv.org/pdf/1905.01116.pdf

[Vallet2017] A noise-immune cavity-assisted non-destructive detection for an optical lattice clock in the quantum regime
G. Vallet, E. Bookjans, U. Eismann, S. Bilicki, R. Le Targat and J. Lodewyck,
New Journal of Physics ***19****, 083002 (2017)* https://doi.org/10.1088/1367-2630/aa7c84

[Wcisło2016] Experimental constraint on dark matter detection with optical atomic clocks
P. Wcisło, P. Morzyński, M. Bober, A. Cygan, D. Lisak, R. Ciuryło and M. Zawada,
Nature Astronomy ***1****, 0009 (2016)* https://arxiv.org/pdf/1605.05763.pdf

[Wcisło2018] New bounds on dark matter coupling from a global network of optical atomic clocks

P. Wcisło, P. Ablewski, K. Beloy, S. Bilicki, M. Bober, R. Brown, R. Fasano, R. Ciuryło, H. Hachisu, T. Ido, J. Lodewyck, A. Ludlow, W. McGrew, P. Morzyński, D. Nicolodi, M. Schioppo, M. Sekido, R. Le Targat, P. Wolf, X. Zhang, B. Zjawin and M. Zawada,
Science Advances ***4****, eaau4869 (2018)* https://arxiv.org/pdf/1806.04762.pdf

[Zhang2017] Ultrastable silicon cavity in a continuously operating closed-cycle cryostat at 4 K
W. Zhang, J.M. Robinson, L. Sonderhouse, E. Oelker, C. Benko, J.L. Hall, T. Legero, D.G. Matei, F. Riehle, U. Sterr and J. Ye,
Physical Review Letters ***119****, 243601 (2017)* https://arxiv.org/pdf/1708.05161.pdf